Two-photon ionization of hydrogen and hydrogenlike ions: Retardation effects on differential and total generalized cross sections

Viorica Florescu*
Department of Physics and Centre for Advanced Quantum Physics, University of Bucharest, P.O. Box MG-11, 077125 Bucharest-Magurele, Romania

Olimpia Budriga
National Institute for Laser, Plasma and Radiation Physics, P.O. Box MG-36, 077125 Bucharest-Magurele, Romania

Henri Bachau†
Centre des Lasers Intenses et Applications, Université Bordeaux 1, unité mixte de recherche de l'Université Bordeaux 1, du Centre National de la Recherche Scientifique et du Commissariat à l'Énergie Atomique et aux Énergies Alternatives, 33405 Talence Cedex, France
(Received 6 August 2012; published 14 September 2012)

We investigate retardation effects in two-photon ionization from the ground state of low-Z hydrogenic atoms for photon energies ranging from 20 eV to 25 keV, using the general formulas of nonrelativistic second-order perturbation theory, including retardation. Our numerical calculations, including all multipoles, show that, as in the K-shell photoeffect, the electron angular distributions are sensitive to retardation. The deviations from the dipole approximation are mainly determined by the terms linear in photon momentum. We also present results for the total generalized cross section along the hydrogen isoelectronic series (for $Z = 1$–5) at scaled laser frequencies.

DOI: 10.1103/PhysRevA.86.033413 PACS number(s): 32.80.Wr, 12.20.Ds

I. INTRODUCTION

Recently available sources in the extreme ultraviolet (EUV) and x-ray photon energy range, such as free electron lasers (FELs), allow the study of processes involving x rays at high intensity and short pulse durations [1]. An example of application is the recent implementation of an x-ray laser in the keV energy regime. The lasing process is based on atomic population inversion driven by rapid K-shell photoionization, using pulses from an x-ray FEL [2]. As long as the intensity of the radiation is not too high, which is the case here, one-photon ionization is the dominant process. Nevertheless, experimental studies show evidence of ionization processes involving the direct absorption of more than one photon in the EUV domain [3,4]. Three recent calculations have explored quantitatively two-photon ionization of the hydrogen atom, two investigations being based on perturbation theory [5,6], the third one on the solution of the time-dependent Schrödinger equation (TDSE) [7]. In the latter work retardation is included and evidence is given that for keV photon energies, the dipole approximation (DA) provides accurate values for the two-photon ionization generalized total cross section and electron energy distribution. Nevertheless, retardation effects modify the electron angular distributions; in the monochromatic case the odd-order multipole contribution vanishes after angular integration, explaining why these effects are not reflected in the electron energy spectra and total ionization cross sections.

Our objective is to pursue our previous investigation [6] of two-photon ionization of the hydrogen atom and hydrogenic ions (fixed nucleus with charge Z) from the fundamental state at energies starting from the photoelectric threshold and up to the x-ray domain. In our study we consider monochromatic radiation and use second-order perturbation theory. In this approach the calculations (numerical or analytic) performed up to now have belonged to one of the following four categories: (i) the nonrelativistic dipole approximation (NRDA), (ii) nonrelativistic with retardation only partially included, (iii) nonrelativistic including the full retardation, and (iv) exact relativistic.

Most of the investigations have been devoted to the calculation of total generalized cross sections. Formalism (i) leads to the precise calculations of Karule [8] (see Ref. [9] for a synthesis). These calculations covered the low-frequency range, up to 620 eV. Results extending up to 50 keV (to be used with caution above 20 keV if more than 2–3 % relative precision is needed) have been published recently (see Table I in Ref. [6]). They are based on approach (ii), briefly described in Sec. II.

Concerning angular distributions associated with two-photon absorption, accurate calculations have been performed more than 40 years ago within the DA [10,11], providing data in the infrared regime. Regardless of the process investigated, electron distributions are in general much more sensitive to approximations than the total cross section is, and here we also expect retardation effects to be more visible in the electron angular distribution.

Our present calculation is done within approach (iii), based on the pioneering work of Klarsfeld [12] and Gavrila [13,14] (for Compton scattering). The analytical equations developed by Gavrila [14] are used here.

Approach (iv), the full relativistic treatment [15], is based on the partial wave expansion of the relativistic Green's function and of the final electron continuum bispinor. The multipolar expansion of the radiation field is also used.

*flor@barutu.fizica.unibuc.ro
†bachau@celia.u-bordeaux1.fr

This approach leads to complicated analytic results expressed as multiple series whose terms are radial double integrals evaluated numerically. More details are given by Koval *et al.* [16], who present the results of a numerical evaluation of the electron angular distribution for atomic numbers $Z = 1$, 54, and 92 in Figs. 2 and 3 of Ref. [16] for a photon energy as low as $1.4E_{2\gamma}$, where $E_{2\gamma}$ is the two-photon ionization threshold.

For low atomic number Z and in the EUV and x-ray domains, it is justified to use the nonrelativistic approach including retardation and not the full relativistic results. Such an approach was adopted in the recent above-mentioned calculations [7], having the merits of calculating the whole electron energy spectrum (beyond one-photon absorption) and the potential of investigating nonperturbative processes.

It is worth noting that retardation effects have been thoroughly studied for the case of one-photon ionization of atoms [17]. In the case of two-photon transitions we mention previous work on two-photon absorption of hydrogen in bound-bound transitions [18,19] and K-shell Rayleigh scattering [20]. A very recent work based on the relativistic approach [21] shows important deviations from the DA angular photon distribution in K-shell Rayleigh scattering.

Our present work follows a previous paper [6] in which we calculated nonrelativistic two-photon ionization cross sections in lowest-order perturbation theory, using approach (ii), i.e., retardation effects included only in the term $\mathbf{A}^2$, while the $\mathbf{A}\cdot\mathbf{P}$ term was treated in the DA ($\mathbf{A}$ is the vector potential in the Coulomb gauge and $\mathbf{P}$ is the momentum operator). In the present calculations retardation is included in both terms and a fully analytic expression is used for the two-photon transition amplitude. This allows for the evaluation of the contribution of each of these two terms. A direct comparison with TDSE results, covering a broad range of photon frequencies, shows remarkable agreement between the lowest-order perturbation theory and TDSE approaches [7,22].

We describe the structure of the analytic formulas for the transition amplitude and the generalized differential cross sections in Secs. II and III, respectively. Section IV gives the relevant equations for the total generalized cross sections. Numerical results are presented in Sec. V, mainly for the electron angular distributions. Our conclusions are summarized in Sec. VI. Appendix A gives details on the analytic formulas, based on Ref. [14], and Appendix B gives analytic expressions for the first-order, linear in photon momentum, corrections to the DA.

II. THEORETICAL APPROACH

We consider here the case of a hydrogenlike atom with a fixed nucleus of charge $-Ze$ ($e < 0$ is the electron charge). In the nonrelativistic formalism, with retardation included, the expression of the two-photon ionization amplitude, obtained in second-order time-dependent perturbation theory, is

$$\mathcal{M}_{\rm NR}^{\rm ret} = \langle E\mathbf{n} - |e^{(2i/\hbar)\boldsymbol{\kappa}\cdot\mathbf{r}}\mathbf{s}^2 - \frac{2}{m}e^{(i/\hbar)\boldsymbol{\kappa}\cdot\mathbf{r}}\mathbf{s}\cdot\mathbf{P} \times G(E_1+\hbar\omega+i\epsilon)\mathbf{s}\cdot\mathbf{P}e^{(i/\hbar)\boldsymbol{\kappa}\cdot\mathbf{r}}|E_1\rangle, \quad \epsilon\to 0^+, \quad (1)$$

where m denotes the electron mass, E_1 is the initial electron energy, $\boldsymbol{\kappa}$ is the photon momentum, $\hbar\omega$ is its energy, and G is the Coulomb Green's function. The emitted electron has an energy E and an asymptotic direction characterized by the unity vector $\mathbf{n}$; the corresponding energy eigenfunction $\langle\mathbf{r}|E\mathbf{n}-\rangle$ is normalized on the energy and solid angle scales and it has the ingoing asymptotic behavior. The photon polarization vector $\mathbf{s}$ is normalized as $\mathbf{s}^*\cdot\mathbf{s} = 1$; it is real for linear polarization, otherwise it is complex.

The ejected electron energy E is

$$E = E_1 + 2\hbar\omega, \quad (2)$$

with $\omega \geqslant \frac{|E_1|}{2\hbar}$, $E_1 = -\frac{\lambda^2}{2m}$, $\lambda = \alpha Zmc$, where c is the velocity of light and α is the fine-structure constant.

The two-photon absorption threshold $E_{2\gamma}$ is half of the photoelectric threshold $|E_1|$. For photon energies ranging from two-photon to one-photon (photoelectric) ionization thresholds, ionization is energetically allowed through the absorption of at least two photons. Above the second threshold one- and two-photon ionization are both possible. As for light elements the threshold for two-photon ionization is low (it is about 1 keV for $Z = 13$), it is usually considered that two-photon ionization just above threshold is well described in the DA. Our calculation shows that the latter assumption is valid for the total cross section, but not for the electron angular distributions.

In the DA the contribution of the first term in the matrix element given in Eq. (1) (i.e., the $\mathbf{A}^2$ contribution, called the seagull term in the literature of Compton scattering) vanishes; the absorption of low-energy photons is generally calculated by using the second term in Eq. (1), taken in the DA. In order to investigate the higher-energy regime, Varma *et al.* [5] have introduced an approach in which the first term is treated exactly and the second one in the DA. These authors introduced a further approximation in the calculation of the summation over intermediate states in the second-order matrix element involving the coupling term $\mathbf{A}\cdot\mathbf{P}$. Our previous work [6], based on a similar approach but with the second-order matrix element calculated exactly, has shown that $\mathbf{A}^2$ plays a negligible role up to energies of 50 keV in the hydrogen case; this is in contrast with Ref. [5]. Furthermore, recent calculations [7,22] including retardation in both terms in Eq. (1) confirmed that at least for photon energies in the keV range, the term $\mathbf{A}^2$ plays a minor role in retardation effects.

For the transition amplitude, we use the analytic developments of Gavrila [14] for Compton scattering. Since we are interested in the absorption of two photons of momentum $\boldsymbol{\kappa}$, we have to use $-\boldsymbol{\kappa}_2 = \boldsymbol{\kappa}_1 = \boldsymbol{\kappa}$ in Gavrila's equations (in the case of radiation scattering $\boldsymbol{\kappa}_1$ is the absorbed photon momentum and $\boldsymbol{\kappa}_2$ is the emitted photon momentum).

In the following it is convenient to use the dimensionless transition amplitude

$$M_{\rm NR}^{\rm ret} = \sqrt{mc^2}\,\mathcal{M}_{\rm NR}^{\rm ret}. \quad (3)$$

The structure of the transition amplitude including the photon polarization vector $\mathbf{s}$ is the same as in Eq. (6) in Ref. [6], but with different invariant amplitudes in the second term:

$$M_{\rm NR}^{\rm ret} = M_{\mathbf{A}^2} + M_{\mathbf{A}\cdot\mathbf{P}}^{\rm ret}, \quad (4)$$

$$M_{\mathbf{A}^2} = O^{\rm abs-two}\mathbf{s}^2, \quad M_{\mathbf{A}\cdot\mathbf{P}}^{\rm ret} = -2[P^{\rm ret}\mathbf{s}^2 + T^{\rm ret}(\mathbf{s}\cdot\mathbf{n})^2]. \quad (5)$$

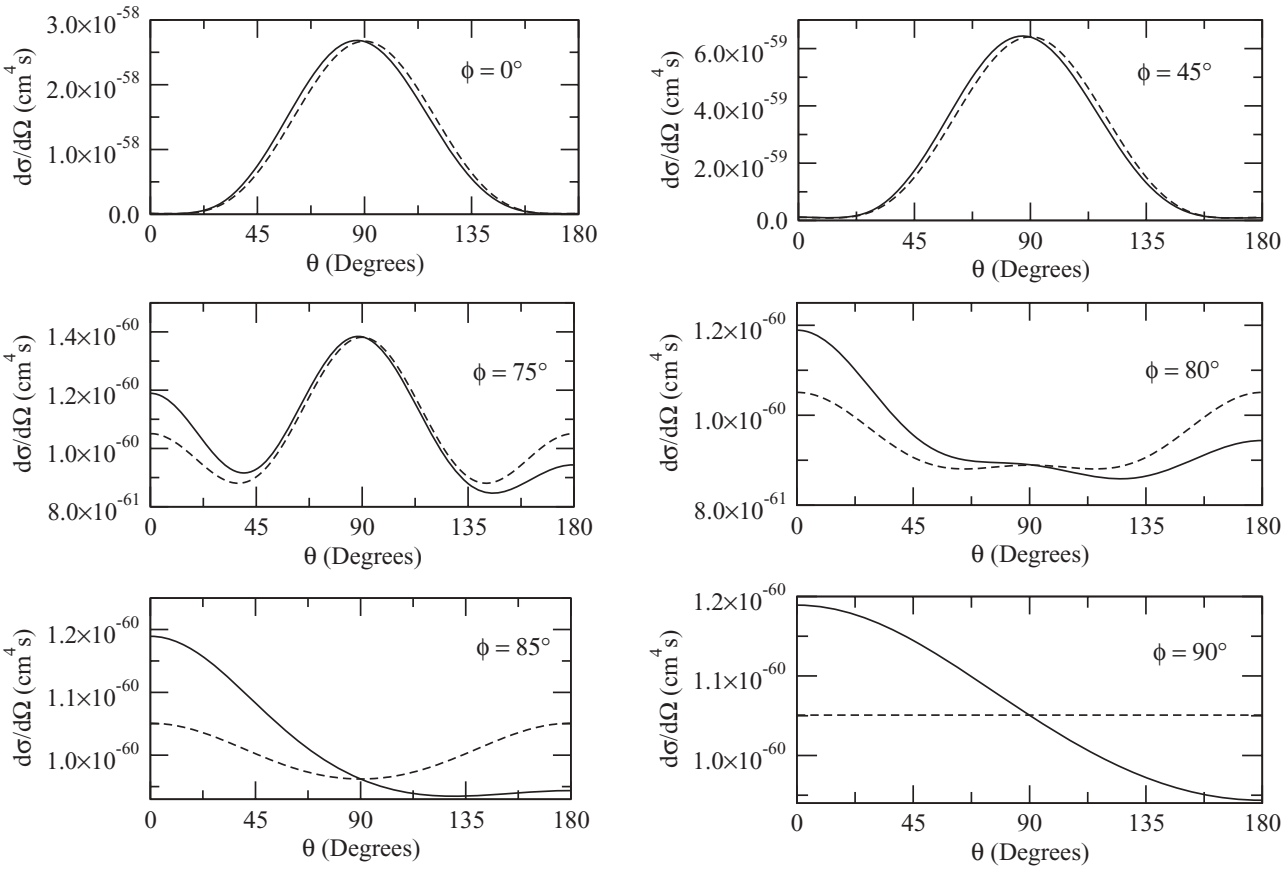

FIG. 1. The GDCS as a function of the polar angle θ of the electron for six values of the azimuthal angle ϕ: comparison between results including full retardation (full line) and DA results (dashed line) in the case $Z = 1$, at 200 eV incident photon energy.

The amplitude denoted by $O^{\text{abs-two}}$ is obtained from the quantity $\mathcal{O}^{\text{abs-two}}$ in Ref. [6] by multiplying by $\sqrt{mc^2}$ and using Eqs. (B2), (B3), and (A7) of the cited reference. The functions denoted here by P^{ret} and T^{ret} are obtained from the amplitudes $\mathcal{P}$ and $\mathcal{T}$ given by Eqs. (48) and (52) of Ref. [14], respectively, through the change of momenta mentioned before and by multiplication with the factor $\sqrt{mc^2}$. For the sake of completeness, the expressions of the amplitudes P^{ret} and T^{ret} are reproduced in Appendix A.

We introduce the invariant amplitude S^{ret} defined by

$$S^{\text{ret}} \equiv O^{\text{abs-two}} - 2P^{\text{ret}} = S_{\mathbf{A}^2} + S^{\text{ret}}_{\mathbf{A}\cdot\mathbf{P}},$$
$$S_{\mathbf{A}^2} = O^{\text{abs-two}}, \quad S^{\text{ret}}_{\mathbf{A}\cdot\mathbf{P}} = -2P^{\text{ret}}. \tag{6}$$

The total amplitude (4) can now be written in terms of the dimensionless invariant amplitudes S^{ret} and T^{ret}:

$$M^{\text{ret}}_{\text{NR}} = S^{\text{ret}}\mathbf{s}^2 - 2T^{\text{ret}}(\mathbf{s}\cdot\mathbf{n})^2. \tag{7}$$

In the dipole approximation only the $\mathbf{A}\cdot\mathbf{P}$ term contributes:

$$M^{\text{DA}}_{\text{NR}} = -2P^{\text{DA}}\mathbf{s}^2 - 2T^{\text{DA}}(\mathbf{s}\cdot\mathbf{n})^2, \tag{8}$$

where the expressions of P^{DA} and T^{DA} are given in Eqs. (B2)–(B4) of the present paper.

Starting from the transition rate $d\Gamma = |\mathcal{M}^{\text{ret}}_{\text{NR}}|^2 d\Omega$, we calculate a *generalized differential cross section* (GDCS) independent of the photon flux J,

$$d\sigma = \frac{d\Gamma}{J^2}, \tag{9}$$

leading to a generalized cross section with the dimension L^4T. The GDCS is then written as

$$d\sigma^{\text{ret}}_{\text{NR}} = \sigma_0\left(\frac{mc}{\kappa}\right)^2 |M^{\text{ret}}_{\text{NR}}|^2 d\Omega_{\mathbf{n}}, \quad \sigma_0 = 2\pi^3\alpha^2\frac{\hbar^5}{m^5c^6}, \tag{10}$$

where the quantity σ_0 bears the dimension of the generalized cross section. The results will be given in cm^4 s; in these units $\sigma_0 \approx 9.4586 \times 10^{-66}$. In the GDCS one distinguishes the three contributions,

$$d\sigma^{\text{ret}}_{\text{NR}} = d\sigma_{\mathbf{A}^2} + d\sigma^{\text{ret}}_{\mathbf{A}\cdot\mathbf{P}} + d\sigma_{\text{interf}}. \tag{11}$$

III. ELECTRON ANGULAR DISTRIBUTION

In order to describe the electrons angular distribution, we use a Cartesian system of reference with the z axis taken along the direction of $\boldsymbol{\kappa}$ (the initial photon momentum) and we denote by θ the angle between the electron momentum $\mathbf{p}$ and $\boldsymbol{\kappa}$. The other two axes are taken along the main axes of the ellipse associated with the photon polarization, with unit vectors $\mathbf{e}_x$ and $\mathbf{e}_y$. The azimuthal angle of the electron momentum is denoted by ϕ. The amplitudes $O^{\text{abs-two}}$, P^{ret}, and T^{ret} depend

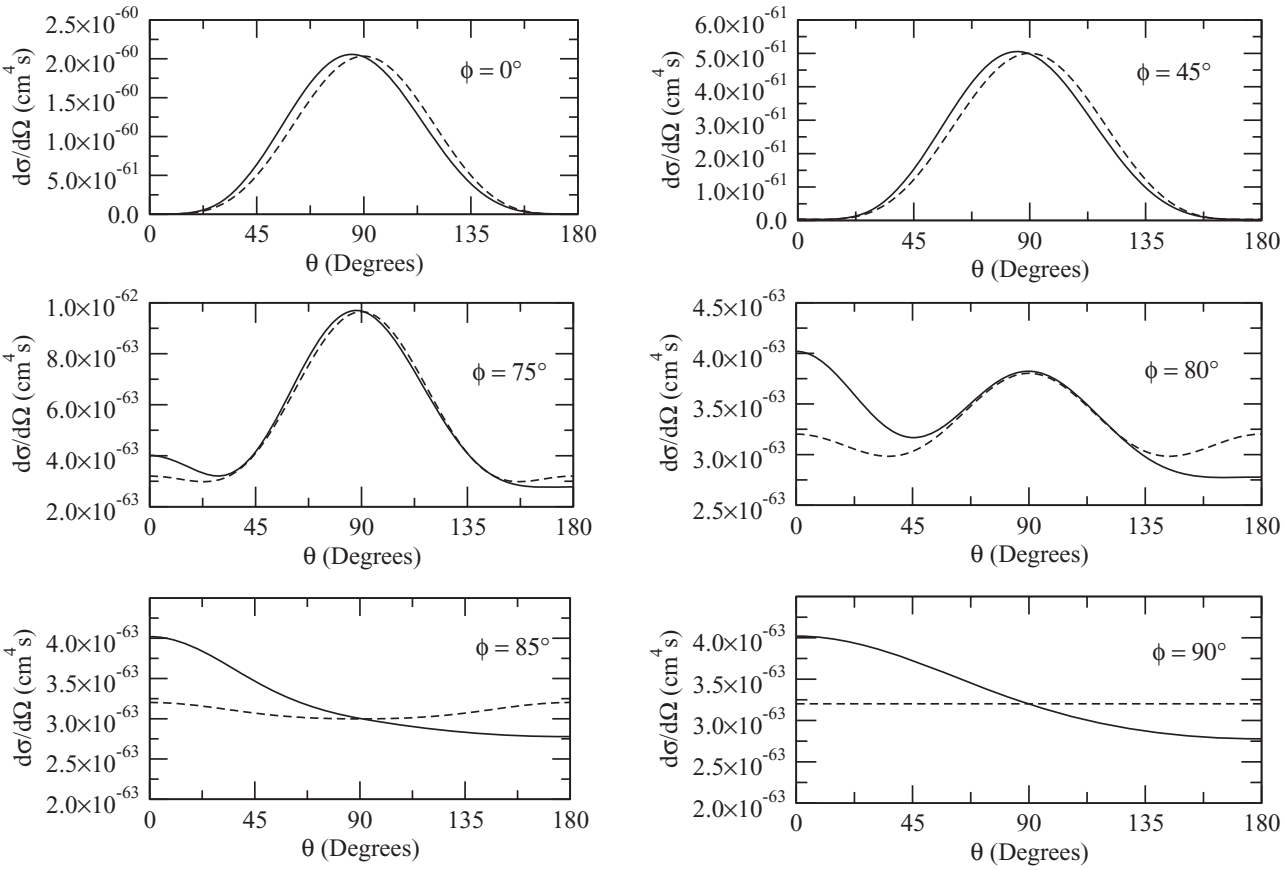

FIG. 2. Same as Fig. 1, but for $Z = 1$ and 0.5 keV.

only on the angle θ. The polarization vector is written

$$\mathbf{s} = \cos\left(\frac{\zeta}{2}\right)\mathbf{e}_x + i\sin\left(\frac{\zeta}{2}\right)\mathbf{e}_y. \tag{12}$$

For $\zeta = 0\,(\pi)$ the photon is linearly polarized along the x (y) axis and $\zeta = \pm\pi/2$ describe circular polarization. We shall use $\zeta = 0$ for linear polarization. Given Eq. (12), it is easy to show that

$$\begin{aligned} \mathbf{s}^2 &= \cos\zeta, \\ (\mathbf{s}\cdot\mathbf{n})^2 &= [\cos(\phi+\zeta/2)\cos(\phi-\zeta/2) \\ &\quad + \frac{i}{2}\sin\zeta\,\sin(2\phi)]\sin^2\theta. \end{aligned} \tag{13}$$

Then the differential cross section is written

$$\begin{aligned} d\sigma_{\rm NR}^{\rm ret} &= \sigma_0\left(\frac{mc}{\kappa}\right)^2 [B(\theta) + C(\theta,\phi)\sin^2\theta \\ &\quad + D(\theta,\phi)\sin^4\theta]d\Omega_{\mathbf{n}}, \end{aligned} \tag{14}$$

$$B(\theta) = |S^{\rm ret}|^2\cos^2\zeta, \tag{15}$$

$$\begin{aligned} C(\theta,\phi) = \{&-4\,{\rm Re}[S^{\rm ret^*}T^{\rm ret}]\cos(\phi+\zeta/2)\cos(\phi-\zeta/2) \\ &+ 2{\rm Im}[S^{\rm ret^*}T^{\rm ret}]\sin\zeta\,\sin(2\phi)\}\cos\zeta, \end{aligned} \tag{16}$$

$$\begin{aligned} D(\theta,\phi) = 4|T^{\rm ret}|^2\big[&\cos^2(\phi+\zeta/2)\cos^2(\phi-\zeta/2) \\ &+ \tfrac{1}{4}\sin^2\zeta\,\sin^2(2\phi)\big]. \end{aligned} \tag{17}$$

Since the invariant amplitudes $S^{\rm ret}$ and $T^{\rm ret}$ depend only on θ, the dependence on ϕ is explicit in the above expressions.

For linear polarization ($\zeta = 0$), $B(\theta)$, $C(\theta,\phi)$, and $D(\theta,\phi)$ are denoted by B_L, C_L, and D_L, respectively, with

$$B_L = |S^{\rm ret}|^2 \equiv b_L(\theta), \tag{18}$$

$$C_L = c_l(\theta)\cos^2\phi, \quad c_L(\theta) = -4\,{\rm Re}[S^{\rm ret^*}T^{\rm ret}], \tag{19}$$

$$D_L = d_L(\theta)\cos^4\phi, \quad d_L(\theta) = 4|T^{\rm ret}|^2. \tag{20}$$

In fact, b_L, c_L, and d_L are functions of $\cos\theta$.

For circular polarization ($\zeta = \pi/2$), the angular distribution does not depend on ϕ as B and C vanish and D becomes equal to D_c, a quantity independent of ϕ,

$$B_c = C_c = 0, \quad D_c = |T^{\rm ret}|^2. \tag{21}$$

The three separate contributions to the cross section, expressed in Eq. (11), follow directly. The contribution of $\mathbf{A}^2$ is simply

$$d\sigma_{\mathbf{A}^2} = \sigma_0\left(\frac{mc}{\kappa}\right)^2 |O^{\rm abs-two}|^2\cos^2\zeta\, d\Omega_{\mathbf{n}}. \tag{22}$$

The contribution of $\mathbf{A}\cdot\mathbf{P}$ to B and C is obtained by replacing $S^{\rm ret}$ by $S^{\rm ret}_{\mathbf{A}\cdot\mathbf{P}}$ in Eqs. (15) and (16). The term D contributes only to $\sigma_{\mathbf{A}\cdot\mathbf{P}}$. The interference term is contained in B and C and is given by the terms linear in $S_{\mathbf{A}^2}$ [see Eq. (6)].

In the DA the previous expressions are applicable with $S^{\rm ret}$ and $T^{\rm ret}$ replaced by $-2P^{\rm DA}$ and $T^{\rm DA}$, respectively. As they are independent of θ, the quantities B, C, and D become

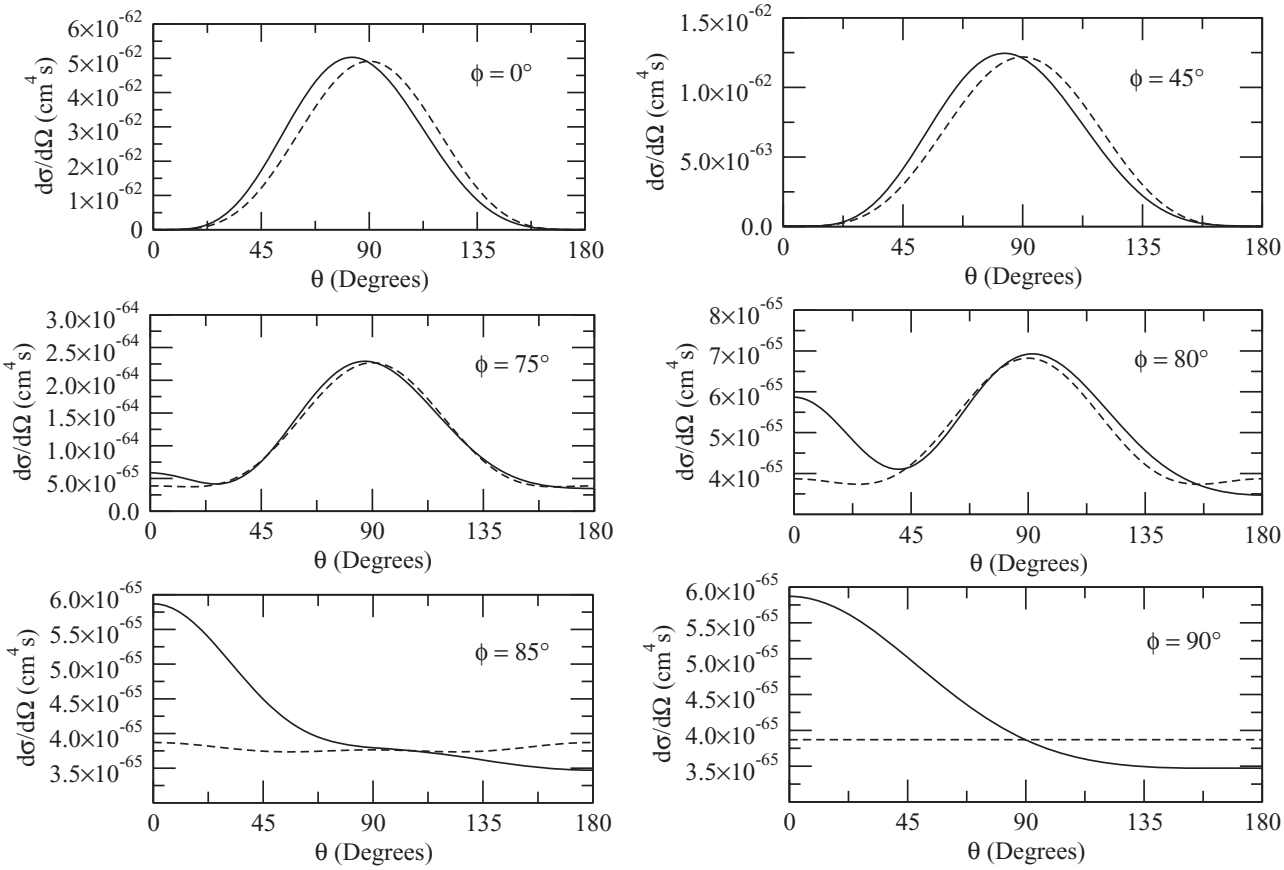

FIG. 3. Same as Fig. 1, but for $Z = 1$ and 1 keV.

independent of θ, so Eq. (14) makes explicit the dependence on θ,

$$d\sigma_{\rm NR}^{\rm DA} = \sigma_0\left(\frac{mc}{\kappa}\right)^2 [B^{\rm DA} + C^{\rm DA}(\phi)\sin^2\theta + D^{\rm DA}(\phi)\sin^4\theta]d\Omega_{\mathbf{n}}. \quad (23)$$

The analytic expressions of the invariant amplitudes with retardation included, given in Appendix A, show that the first retardation corrections in the GDCS are linear in photon momentum. We present these corrections in Appendix B.

Here it is worth noting that in order to make a comparison with others works, the definition of the reference axes for the angles must be carefully checked. For example, in the case of linear polarization, according to Eq. (12) with $\zeta = 0$, we have taken the x axis along the polarization vector. Our choice of axes is different from that used in Refs. [7,12], where the calculation was done for the z axis along the polarization vector and the x axis along the photon direction. Denoting by θ' and ϕ' the polar angles of the electron momentum for this alternative choice of the reference system, the connection with the angle θ and ϕ defined above is given by

$$\cos\theta' = \sin\theta\cos\phi, \quad \sin\theta'\cos\phi' = \cos\theta. \quad (24)$$

IV. TOTAL CROSS SECTIONS

In order to obtain the total cross section we start from Eqs. (14)–(17); noting that the integration over the polar angle ϕ is elementary, we are left with a distribution depending only on the polar angle θ, with the corresponding generalized cross section denoted by $\widetilde{d\sigma}_{\rm NR,ret}$,

$$\widetilde{d\sigma}_{\rm NR,ret} = 2\pi\sigma_0\left(\frac{mc}{\kappa}\right)^2\left\{(|S^{\rm ret}|^2 - 2\,{\rm Re}[S^{\rm ret^*}T^{\rm ret}]\sin^2\theta) \times \cos^2\zeta + \frac{|T^{\rm ret}|^2}{2}(3-\sin^2\zeta)\sin^4\theta\right\}\sin\theta d\theta. \quad (25)$$

For linear polarization the formula reads

$$\widetilde{d\sigma}^{\,L}_{\rm NR,ret} = 2\pi\sigma_0\left(\frac{mc}{\kappa}\right)^2\left\{|S^{\rm ret}|^2 - 2\,{\rm Re}[S^{\rm ret^*}T^{\rm ret}]\sin^2\theta + \tfrac{3}{2}|T^{\rm ret}|^2\sin^4\theta\right\}\sin\theta d\theta \quad (26)$$

and for circular polarization

$$\widetilde{d\sigma}^{\,C}_{\rm NR,ret} = 2\pi\sigma_0\left(\frac{mc}{\kappa}\right)^2|T^{\rm ret}|^2\sin^5\theta d\theta. \quad (27)$$

In order to calculate the total generalized cross section (GCS), the integration of the GDCS over θ given in Eq. (25) has to be performed numerically. In the DA this operation can be done analytically and the result

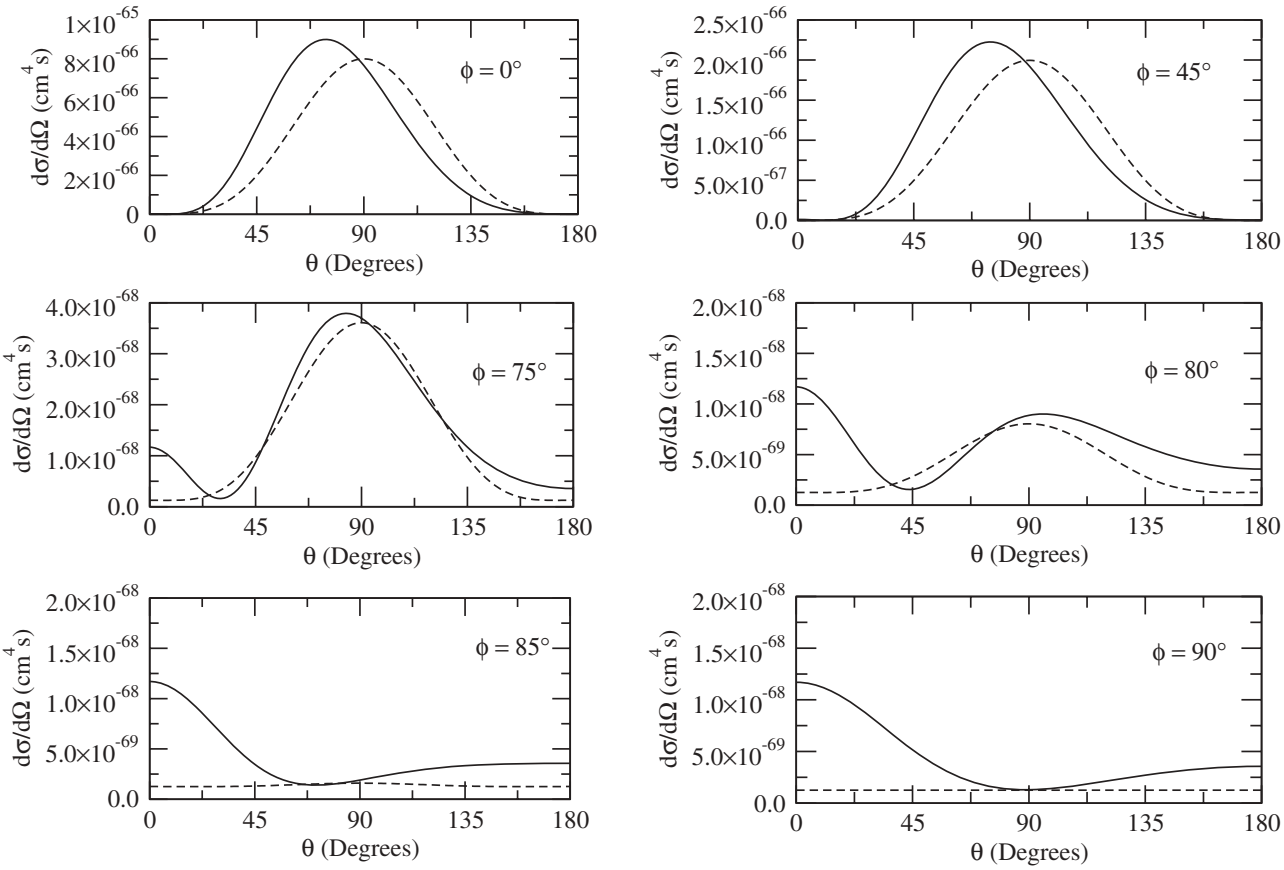

FIG. 4. Same as Fig. 1, but for $Z = 1$ and 5 keV.

reads

$$\sigma_{\rm NR}^{\rm DA} = 16\pi\sigma_0\left(\frac{mc}{\kappa}\right)^2\left\{\left(|P^{\rm DA}|^2 + \frac{2}{3}{\rm Re}[P^{\rm DA^*}T^{\rm DA}]\right)\cos^2\zeta + \frac{3-\sin^2\zeta}{15}|T^{\rm DA}|^2\right\}. \quad (28)$$

When integrating over θ the contribution of the odd powers of $\boldsymbol{\kappa}\cdot\mathbf{r}$ in a multipolar expansion of the exponential in Eq. (1) disappear. Therefore, the lowest-order retardation correction to the GCS is of second order in photon momentum, thus less important than in the case of GDCS.

V. NUMERICAL RESULTS

Numerical values for nonrelativistic generalized differential cross sections that include retardation are unavailable, in contrast to the DA case. In this context, as an approximate check, we have compared our results with the data of Koval *et al.*, presented in Fig. 2 of Ref. [16], which are based on a *relativistic treatment*. The published relativistic results refer to linear, circular, and unpolarized incident photons, for an azimuthal angle of the electron $\phi = 0$, in the case of hydrogenic atoms with $Z = 1, 54$, and 92 and a photon energy of $0.7|E_1|$. The photon energy, corresponding to $\tau \approx 1.83$ [the definition of τ is given in Eq. (A12)], is low from the point of view of our codes, which give reliable results provided $\tau < 1$. Nevertheless, it is possible to transform the two Lauricella functions in Eq. (A4) in order to extend the range of validity of our codes regarding the value of τ. The transformation consists in integrating by parts the integrand that represents the Lauricella function in Eq. (A13). We should remark that the agreement we have found at $Z = 1$ is irrelevant for our purpose because the retardation effects are totally negligible

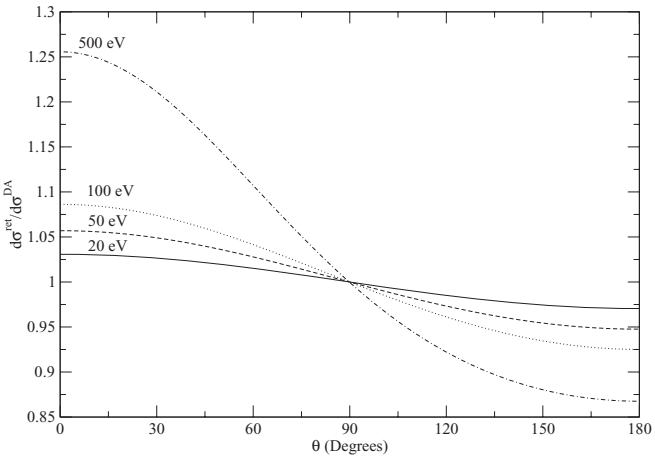

FIG. 5. Ratio of the GDCS with retardation included and the GDCS in the dipole approximation as a function of the polar angle θ of the electron at the azimuthal angle $\phi = \pi/2$, for $Z = 1$, linear polarization, and different photon energies as marked on the curves.

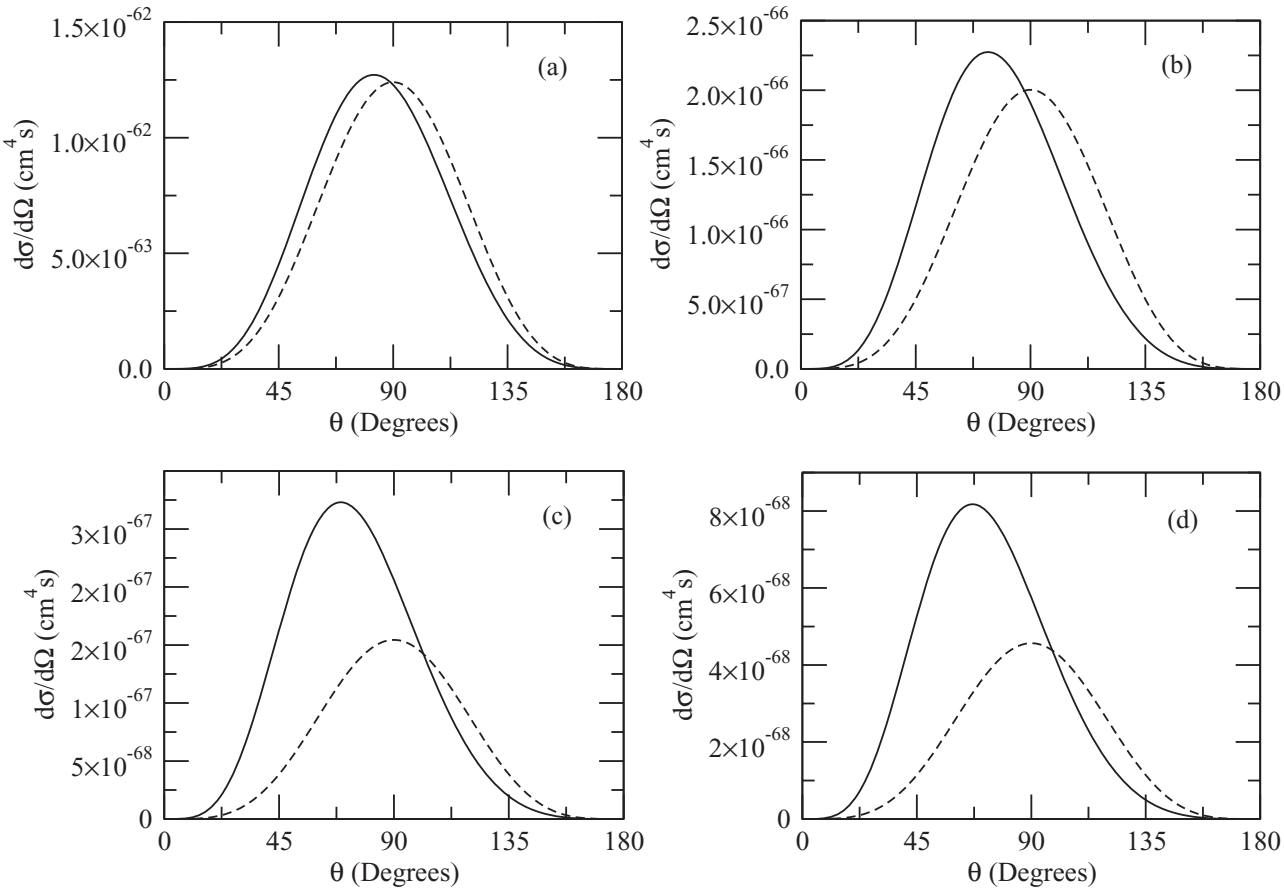

FIG. 6. The GDCS as a function of the polar angle θ of the electron in the case of circularly polarized photons for $Z = 1$ and different photon energies: (a) 1 keV, (b) 5 keV, (c) 8 keV, and (d) 10 keV. The DA results are represented by dashed lines.

in the present case due to very low energy (9.52 eV) of the photons. At $Z = 54$, where we do not expect agreement, we find relative differences up to 25%, but a similar behavior, i.e., the effect of retardation is a shift of the angular distribution towards a smaller angle and an increase of its values. We remark that in the case of linear polarization we find the same position of the maxima as in Fig. 2 of Ref. [16]: 72° and 61° for $Z = 54$ and 92, respectively. Similar agreement holds for circular polarization. Also, the dependence of the azimuthal angle is in qualitative agreement with that displayed in Fig. 3 of Ref. [16] for $Z = 92$.

We present our results for the angular differential generalized cross section (GDCS) in Figs. 1–6. In Figs. 1–4, which refer to *linear polarization* of the absorbed photons, for the case of the hydrogen atom, each of the six panels presents the angular distribution of the electron as a function of the polar angle θ, for a fixed value of the azimuthal angle ϕ. Figures 1–4 correspond to the photon energies 0.2, 0.5, 1, and 5 keV, respectively. In these figures we can follow the change of the shape of the angular distribution (solid line) when compared with the DA curve (dashed line). The DA curve is always symmetric with respect to $\theta = \pi/2$, in accordance with Eq. (23). From a quasisymmetric shape at $\phi = 0$ with the maximum near $\theta = \pi/2$, the shape changes gradually: At $\phi = 85°$ there is no maximum anymore; at 200 eV the corrections to the DA are already of the order of 10%. Differences are already present at a 20-eV energy of the photons, as shown in Fig. 5.

The situation at $\phi = \pi/2$ is the most interesting because in this case there is no θ dependence in the DA. With retardation included, we see from Eq. (18) that only the amplitude B_L is different from 0, so we have

$$\frac{d\sigma^{\rm ret}}{d\Omega}(\theta,\phi = \pi/2) = |S^{\rm ret}|^2. \tag{29}$$

An examination of the graphs corresponding to $\phi = \pi/2$ for $Z = 1$ and energies of 200 and 500 eV and 1 keV (Figs. 1–3) shows that the deviation from the DA is positive for $\theta < \pi/2$, vanishes at $\theta = \pi/2$, and becomes negative for $\theta > \pi/2$. This reveals mainly linear retardation effects in the amplitude $S^{\rm ret}$ [defined in Eq. (6)], due to the terms proportional to $\boldsymbol{\kappa} \cdot \mathbf{p} = \kappa p \cos\theta$. The analytic expressions of the correction terms is given in Eqs. (B11) and (B12). At higher energies (5 keV in Fig. 4), the change of sign at $\phi = \pi/2$ is not present anymore, which proves the presence of quadratic effects in the photon momentum. At $Z = 1$, 1 keV (Fig. 3), $\phi = \pi/2$, and $\theta = 0$, the relative difference of the retarded results with respect to the DA results reaches almost 50%.

With increasing photon energy, retardation effects become important and visible even at $\phi = 0$. This is illustrated in Fig. 4 for $\hbar\omega = 5$ keV, where the first panel shows that the maximum is shifted to $\theta \approx 74°$. Also, the trend with θ at $\phi \geqslant 80°$ is

different from in previous figures; the results (with retardation included) are now always larger than the DA values. For $\phi = \pi/2$ and $\theta = 0$, the relative difference is as big as 8.3. This proves here also that the terms quadratic in photon momentum become important.

In Fig. 5 we describe in more detail the case of linear polarization with $Z = 1$ and $\phi = \pi/2$ by plotting the ratio of the nonrelativistic with retardation and the DA values of the GDCS as a function of θ for several incident photon energies. The deviations from 1 measure the retardation effects and their dependence on θ shows the dominance of the corrections proportional to $\boldsymbol{\kappa} \cdot \mathbf{p}$ described in Appendix B.

In the case of circularly polarized photons, according to Eqs. (14) and (21), there is no ϕ dependence in the GDCS, so for each photon energy there is only one angular distribution attached. The amplitude $T^{\rm ret}$ solely determines the values of the distribution. In Fig. 6 we show the results obtained for $Z = 1$ for photon energies of 1, 5, 8, and 10 keV. The behavior is similar to that found at $\phi = 0$ in the linear polarization case, only the GDCS values are now larger.

As noticed in Sec. II and displayed in Eq. (14), the two-photon ionization cross sections are determined by two complex functions, the amplitudes $S^{\rm ret}$ and $T^{\rm ret}$, which depend on three variables: the ion charge Z, the photon energy $\hbar\omega = \kappa/c$, and the final electron polar angle θ. This means that all needed information for calculating the GDCS would be tables or graphs of these two amplitudes, as a function of θ for the photon energies of interest. As an illustration we present Figs. 7 and 8 for $Z = 1$. Figure 7 corresponds to a 500-eV photon energy; it contains not only the real and imaginary parts of the amplitude $S^{\rm ret}$, but also the terms $O^{\rm abs-two}$ and $P^{\rm ret}$ from which $S^{\rm ret}$ is built, according to its definition given in Eq. (6). Figure 8 refers to the amplitude $T^{\rm ret}$. Here two energies (500 eV and 1 keV) are considered. By comparing the amplitudes at 500 eV in Figs. 7 and 8, one sees that at this photon energy Re$[T^{\rm ret}]$ is approximately 14 times larger than Im$[S^{\rm ret}]$, which explains why in the circular polarization case we find larger values for the GDCS. Figure 7 shows that the imaginary part of $S^{\rm ret}$ dominates the real part. More important, one sees that the contribution of $O^{\rm abs-two}$ is negligible compared to that of

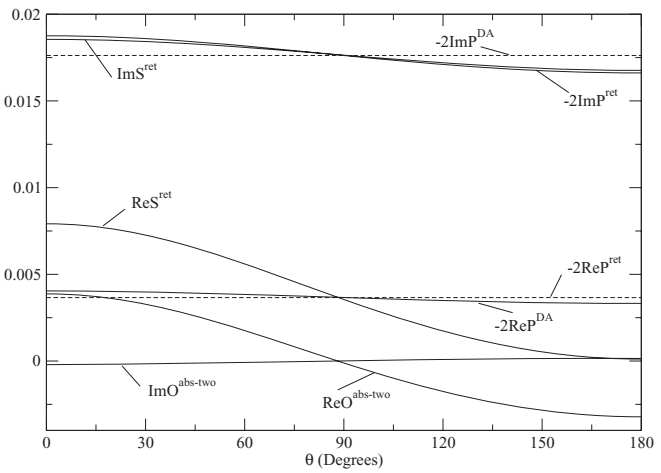

FIG. 7. Real and imaginary parts of the dimensionless amplitudes $S^{\rm ret}, O^{\rm abs-two}$, and $P^{\rm ret}$. Also shown is a comparison with $P^{\rm DA}$, with $Z = 1$ and a photon energy of 500 eV.

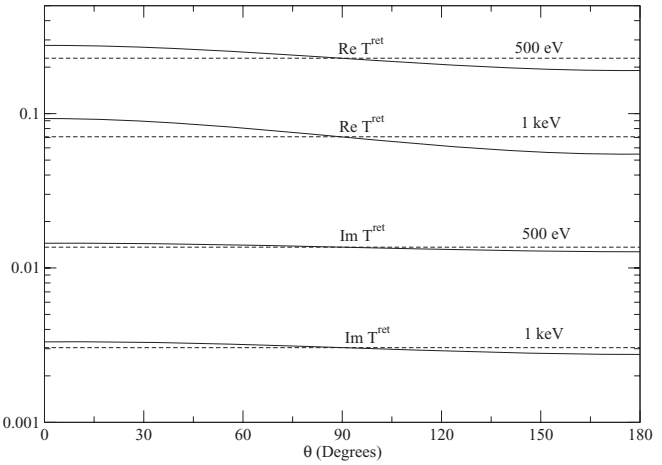

FIG. 8. Real and imaginary parts of the dimensionless amplitude $T^{\rm ret}$ (solid lines). Also shown is a comparison with $T^{\rm DA}$ (dashed lines), with $Z = 1$ and photon energies of 500 eV and 1 keV.

$P^{\rm ret}$; as a consequence, the $\mathbf{A} \cdot \mathbf{P}$ contribution to the DGCS in Eq. (11) is more important than the $\mathbf{A}^2$ contribution.

The final figure regarding GDCS is Fig. 9, which illustrates the validity of the approximate expression for the GDCS based on the inclusion of the corrections brought only by the terms linear in momentum given in Appendix B. The ratio between the approximate result for the GDCS that includes only the corrections linear in photon momentum and the nonrelativistic results including all multipoles is represented as a function of the angle θ for several photon energies and linear polarization.

We have calculated the total GCS by integrating the GDCS given in Eq. (25) over θ. In the DA the cross section $\sigma^{\rm DA}_{\mathbf{A}\cdot\mathbf{P}}$, which gives the dominant contribution (at least up to photon energies of 50 keV), follows a simple scaling law in Z [23]: $Z^6\sigma^{\rm DA}_{\mathbf{A}\cdot\mathbf{P}}(Z,\omega) = \sigma^{\rm DA}_{\mathbf{A}\cdot\mathbf{P}}(1,\omega/Z^2)$. In the relativistic calculation presented in Ref. [15], the Z dependence of the ratio of the relativistic GCS for the charges Z and 1, multiplied by Z^6, was displayed at two low photon energies. The comparison also

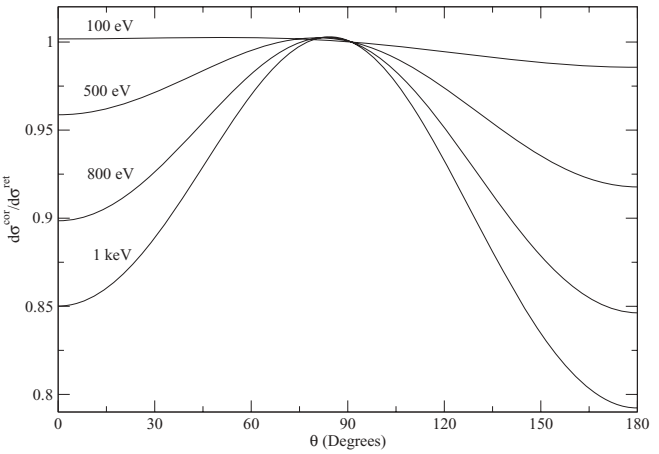

FIG. 9. Ratio of the approximate GDCS (including the DA and the linear correction in photon momentum) and the exact nonrelativistic GDCS including all multipoles, as a function of the polar angle θ of the electron at the azimuthal angle $\phi = \pi/2$ for $Z = 1$. The photon energies are given in the figure.

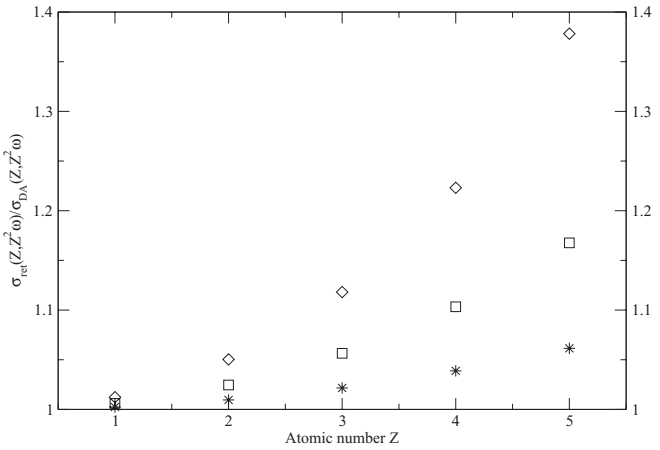

FIG. 10. Ratio of the retarded total cross sections $\sigma_{\rm ret}(Z,Z^2\omega)$ and $\sigma_{\rm DA}(Z,Z^2\omega)$ taken for different nuclear charges Z for three different photon energies $\hbar\omega$: 200 eV (asterisks), 500 eV (squares), and 1 keV (diamonds).

involves a relativistic calculation done in the DA. It indicates that in the case considered, the relativistic effects on the GCS are more important than retardation effects, the latter being practically invisible at $1.05E_{2\gamma}$ (see Fig. 1 of Ref. [15]), but at the higher energy of $1.4E_{2\gamma}$ the indication from Fig. 2 of Ref. [15] is that retardation effects matters. Retardation effects are nevertheless small for $Z < 20$.

Having in mind the scaling law valid in the DA, we represent in Fig. 10, as function of Z, the ratio of the retarded and DA cross sections, both taken at energies $Z^2\hbar\omega$ for three values of the photon energy: $\hbar\omega = 0.2, 0.5$, and 1 keV and linear polarization. The figure clearly shows the effect of retardation for $Z \geqslant 2$ and, as expected, the retardation effect increases with the photon energy. In fact, retaining only the first correction term in the multipole expansion of the exponentials in Eq. (1), it is easy to show that the relative difference between retarded and DA total cross sections varies like Z^2. The latter approximation is valid provided $\alpha\hbar\omega \leqslant Z$ [22] (with $\hbar\omega$ given in a.u.). This is verified over the range of photon energies explored in Fig. 10 (except for the top curve at $Z = 5$) and the three curves agree with the expected Z^2 behavior. Also, the figure shows that for $\alpha\hbar\omega \approx 1$ a.u., the correction due to retardation effects is close to 5% of the DA total cross section.

VI. CONCLUSION

In this work we have investigated retardation effects in two-photon ionization of hydrogen and hydrogenlike ions in lowest-order perturbation theory. The nonrelativistic atomic Hamiltonian has been considered with full retardation included in both $\mathbf{A}\cdot\mathbf{P}$ and $\mathbf{A}^2$ terms. It is possible to express the generalized two-photon ionization differential cross section with a compact expression [Eq. (7)] using two invariant amplitudes $T^{\rm ret}$ and $S^{\rm ret}$, which depend only on the photon energy and polar angle θ between the electron and photon momenta, the azimuthal angle ϕ and the polarization component ζ being explicitly expressed in terms of trigonometric functions. In the case of hydrogen, differential cross sections versus θ are examined for a photon energy range of 200–5000 eV, with linear polarization ($\zeta = 0$). At low photon energies strong deviations with the DA are observed for ϕ close to $\pi/2$, while significant differences appear for all values of ϕ at higher photon energies. The case of $\phi = \pi/2$ is of particular interest since the DA differential cross section is independent of θ; the DA and non-DA results show large differences. Examining the latter case at various photon energies, we note a clear evolution of the θ dependence of the differential cross section: from an asymmetric shape with respect to the vertical axis $\theta = \pi/2$ at a photon energy of 200 eV to a symmetric one at 5 keV. This evolution is clearly related to the influence of quadratic effects in photon momentum, which increases with the photon energy. For a circularly polarized field, the differential cross section does not depend on the azimuthal angle ϕ; the difference between DA and non-DA results is of the order of magnitude of the one observed in linear polarization for $\phi = 0$. Finally, for the total cross section we have studied retardation effects along the isoelectronic series of hydrogen with scaled photon energies. We have noticed that retardation effects become significant for $\alpha\hbar\omega \approx 1$ and rapidly increase with the nuclear charge Z. As the nuclear charge Z increases, an analysis of the relativistic effects is desirable.

ACKNOWLEDGMENTS

This work was initiated in the framework of the European Cooperation in Science and Technology Action No. CM0702. V.F. and O.B. acknowledge the support of the contract project number 1 RNP/2012 from Autoritatea Nationala pentru Cercetare Ştiinţifică through Consiliul National al Cercetarii Stiintifice. Useful discussions with Mihai Dondera are warmly acknowledged.

APPENDIX A: ANALYTIC RESULTS FOR THE A · P CONTRIBUTION

The contribution of the $\mathbf{A}\cdot\mathbf{P}$ term from the nonrelativistic Hamiltonian to the absorption of two identical photons is determined by the two invariant amplitudes $P^{\rm ret}$ and $T^{\rm ret}$ in Eq. (5). Their compact analytic expressions are obtained, as described in Sec. II, from Eqs. (49) and (52) of Ref. [14], respectively, as

$$P^{\rm ret} = c_1\frac{g_1}{2-\tau},$$

$$c_1 = \widetilde{N}\lambda X^3\frac{[(X-ip)^2+\kappa^2]^{-1-i\eta}}{[(X+\lambda)^2+\kappa^2]^2[X^2+(\mathbf{p}-\boldsymbol{\kappa})^2]^{1-i\eta}}, \quad \text{(A1)}$$

$$T^{\rm ret} = c_2\left[\frac{g_2}{2-\tau} - \frac{(X-\lambda)^2+\kappa^2}{(X+\lambda)^2+\kappa^2}\frac{g_3}{4-\tau}\right],$$

$$c_2 = 2\widetilde{N}X^4p^2\frac{(1-i\eta)(2-i\eta)[(X-ip)^2+\kappa^2]^{-i\eta}}{[(X+\lambda)^2+\kappa^2]^2[(X^2+(\mathbf{p}-\boldsymbol{\kappa})^2]^{3-i\eta}}. \quad \text{(A2)}$$

Explanations of the notations follow. The quantity η is introduced by the continuum wave function in the matrix element given in Eq. (1) and the constant factor $\widetilde{N}$ is

$$\widetilde{N} = \frac{32mc}{\pi}(2\lambda^5p)^{1/2}\Gamma(1-i\eta)\exp\left(\frac{\pi}{2}\eta\right),$$
$$\eta = \lambda/p, \quad \lambda = \alpha Zmc, \quad \text{(A3)}$$

where g_1, g_2, and g_3 denote the three Lauricella functions of the type F_D [24],

$$g_1 = F_D(2-\tau;1+i\eta,1+i\eta,1-i\eta,1-i\eta;3-\tau;\xi_1,\xi_2,\xi_3,\xi_4), \tag{A4}$$

$$g_2 = F_D(2-\tau;i\eta,i\eta,3-i\eta,3-i\eta;3-\tau;\xi_1,\xi_2,\xi_3,\xi_4), \tag{A5}$$

$$g_3 = F_D(4-\tau;i\eta,i\eta,3-i\eta,3-i\eta;5-\tau;\xi_1,\xi_2,\xi_3,\xi_4). \tag{A6}$$

For the two variables ξ_1 and ξ_2 the expressions of the sum and the product are given in Eqs. (42) and (43) of Ref. [14], respectively, which we adapt to the case of absorption of two identical photons,

$$\xi_1+\xi_2 = 2\frac{-4\kappa^2X^2+(\lambda^2+\kappa^2-X^2)(\kappa^2-p^2-X^2)}{[(X+\lambda)^2+\kappa^2][(X-ip)^2+\kappa^2]}, \tag{A7}$$

$$\xi_1\xi_2 = \frac{(X-\lambda)^2+\kappa^2}{(X+\lambda)^2+\kappa^2}\frac{(X+ip)^2+\kappa^2}{(X-ip)^2+\kappa^2}. \tag{A8}$$

For the other pair of variables (ξ_3,ξ_4) one gets, from Eqs. (44) and (45) of Ref. [14],

$$\xi_3+\xi_4 = 2\frac{4\boldsymbol{\kappa}\cdot(\mathbf{p}-\boldsymbol{\kappa})X^2+(\lambda^2+\kappa^2-X^2)[(\mathbf{p}-\boldsymbol{\kappa})^2-X^2]}{[(X+\lambda)^2+\kappa^2][X^2+(\mathbf{p}-\boldsymbol{\kappa})^2]}, \tag{A9}$$

$$\xi_3\xi_4 = \frac{(X-\lambda)^2+\kappa^2}{(X+\lambda)^2+\kappa^2}. \tag{A10}$$

As in the DA, the argument Ω of the amplitudes $P^{\rm ret}$ and $T^{\rm ret}$ comes from the Green's function in Eq. (1) and has the expression

$$\Omega = E_1+\hbar\omega+i\epsilon, \quad \epsilon\to 0^+. \tag{A11}$$

It determines the two quantities X and τ in the previous expressions,

$$X^2 = -2m\Omega, \quad \mathrm{Re}X \geqslant 0, \quad \tau = \frac{\lambda}{X}. \tag{A12}$$

Between the two-photon and one-photon thresholds situated, respectively, at $|E_1|/2$ and $|E_1|$, one has $\Omega<0$ and consequently X is real; τ is also real and increases from $\sqrt{2}$ to ∞ from the two-photon to the one-photon thresholds. Above the photoelectric threshold X is purely imaginary, namely, $X=-i|X|$.

The evaluation of the Lauricella functions is done with the same technique as in the DA case [6], using the one-dimensional integral representation of them. A simplification arises from the fact that the functions we have to evaluate are of the particular type

$$\begin{aligned} &F_D(a;b_1,b_1,b_2,b_2;a+1;\xi_1,\xi_2,\xi_3,\xi_4) \\ &\quad = a\int_0^1 \rho^{a-1}[1-(\xi_1+\xi_2)\rho+\xi_1\xi_2\rho^2]^{-b_1} \\ &\qquad \times[1-(\xi_3+\xi_4)\rho+\xi_3\xi_4\rho^2]^{-b_2}d\rho, \\ &\mathrm{Re}a>0, \end{aligned} \tag{A13}$$

i.e., they depend on three independent parameters instead of six. Therefore, in the integrand in Eq. (A13), we meet the sum and the product for each pair of the variables (ξ_1,ξ_2) and (ξ_3,ξ_4) and there is no need to manipulate explicitly these variables. We mention also that the variables are such that there no singularities along the segment [0,1] of the real axis.

For $\tau\geqslant 2$, due to the presence of a singularity at the origin in the integrand representing the function g_1, one or more integrations by parts increase the power at which the variable appears, making the procedure applicable. The limit $\tau=2$ corresponds to a photon energy of $3/4|E_1|$ ($|E_1|$ is the photoeffect threshold).

APPENDIX B: FIRST-ORDER RETARDATION CORRECTIONS TO THE DA ELECTRON ANGULAR DISTRIBUTION

The first corrections to the DA are due to the terms in $\mathbf{p}\cdot\boldsymbol{\kappa}$ present in the analytic expressions of the invariant amplitudes. We make series expansions of the amplitudes and keep only the terms linear in this quantity. Before writing the results, we recall the DA expressions.

The contribution of the $\mathbf{A}^2$ term to the transition amplitude $S^{\rm ret}$, given by $O^{\rm abs-two}$, vanishes in the DA. As shown in Ref. [14], the four variables of the Lauricella functions determining the $\mathbf{A}\cdot\mathbf{P}$ contribution in the DA reduce to two, namely,

$$\xi_1^{\rm DA}=\xi_2^{\rm DA}=\xi_3^{\rm DA}\equiv x, \quad \xi_4^{\rm DA}\equiv y, \tag{B1}$$

with the expressions of x and y given by Eq. (A4) of Ref. [6]. As a consequence, each of the Lauricella functions reduces to an Appell function F_1, leading to

$$\begin{aligned} P^{\rm DA} &= c_1^{\rm DA}\frac{f_1}{2-\tau}, \\ c_1^{\rm DA} &= \widetilde{N}\frac{\tau}{(1+\tau)^4}(X+ip)^{-1+i\eta}(X-ip)^{-3-i\eta}, \end{aligned} \tag{B2}$$

$$T^{\rm DA} = c_2^{\rm DA}\left[\frac{f_2}{2-\tau}-\frac{(X-\lambda)^2}{(X+\lambda)^2}\frac{f_3}{4-\tau}\right], \tag{B3}$$

$$c_2^{\rm DA} = 2\widetilde{N}p^2\frac{(1-i\eta)(2-i\eta)(X+ip)^{-3+i\eta}(X-ip)^{-3-i\eta}}{(1+\tau)^4}. \tag{B4}$$

The three Appell functions involved are

$$f_1 = F_1(2-\tau;3+i\eta,1-i\eta;3-\tau;x,y), \tag{B5}$$

$$f_2 = F_1(2-\tau;3+i\eta,3-i\eta;3-\tau;x,y), \tag{B6}$$

$$f_3 = F_1(4-\tau;3+i\eta,3-i\eta;5-\tau;x,y). \tag{B7}$$

Now we describe the corrections linear in $\boldsymbol{\kappa}\cdot\mathbf{p}$. The $\mathbf{A}^2$ contribution is obtained from Eqs. (B2) and (B3) in Ref. [6] neglecting all $K^2=4\kappa^2$ terms:

$$O^{\rm abs-two}\approx\frac{\widetilde{N}}{4p^2}\frac{\boldsymbol{\kappa}\cdot\mathbf{p}}{(\lambda^2+p^2)^2}\frac{e^{-2\eta\arctan(1/\eta)}}{1+i\eta}. \tag{B8}$$

In the $\mathbf{A}\cdot\mathbf{P}$ term, corrections come from the Lauricella functions and their coefficients. In fact, only two of the four variables of the Lauricella functions in Eq. (A4), namely, ξ_3 and ξ_4, are affected by first-order terms in κ. The sum of these two variables is approximately

$$\xi_3+\xi_4\approx(x+y)+\frac{2\boldsymbol{\kappa}\cdot\mathbf{p}}{p^2+X^2}u_c,$$
$$u_c\equiv\frac{4}{(1+\tau)^2}\frac{2X^2-\lambda^2+p^2}{X^2+p^2}, \tag{B9}$$

while the product of the variables contains terms in κ^2 only. In this particular case, using the integral representation (A13), one derives easily the approximate result

$$\begin{aligned}&F_D(a;b_1,b_1,b_2,b_2;a+1;\xi_1,\xi_2,\xi_3,\xi_4)\\&\quad=F_1(a;2b_1+b_2,b_2;a+1;x,y)+\frac{ab_2}{a+1}\frac{2\boldsymbol{\kappa}\cdot\mathbf{p}}{p^2+X^2}u_c\\&\qquad\times F_1(a+1;2b_1+b_2+1,b_2+1;a+2;x,y).\end{aligned} \tag{B10}$$

The final results for the corrections to the P^{DA} and T^{DA} are

$$P_{\mathrm{cor}}=(1-i\eta)\frac{2\boldsymbol{\kappa}\cdot\mathbf{p}}{p^2+X^2}\left[P^{\mathrm{DA}}+c_1^{\mathrm{DA}}u_c\frac{f_4}{3-\tau}\right], \tag{B11}$$

$$\begin{aligned}T_{\mathrm{cor}}=(3-i\eta)\frac{2\boldsymbol{\kappa}\cdot\mathbf{p}}{p^2+X^2}&\left\{T^{\mathrm{DA}}+c_2^{\mathrm{DA}}u_c\right.\\&\left.\times\left[\frac{f_5}{3-\tau}-\left(\frac{1-\tau}{1+\tau}\right)^2\frac{f_6}{5-\tau}\right]\right\}.\end{aligned} \tag{B12}$$

The three new Appell functions denoted by f_4, f_5, and f_6 are

$$f_4=F_1(3-\tau;4+i\eta,2-i\eta;4-\tau;x,y), \tag{B13}$$

$$f_5=F_1(3-\tau;4+i\eta,4-i\eta;4-\tau;x,y), \tag{B14}$$

$$f_6=F_1(5-\tau;4+i\eta,4-i\eta;6-\tau;x,y). \tag{B15}$$

Finally, we remark that, using the energy conservation law given in Eq. (2), the factor $2\boldsymbol{\kappa}\cdot\mathbf{p}/(p^2+\lambda^2)$ entering the corrections to the $\mathbf{A}^2$ contribution becomes

$$\frac{2\boldsymbol{\kappa}\cdot\mathbf{p}}{p^2+\lambda^2}=\frac{p}{2mc}\cos\theta \tag{B16}$$

and the factor $2\boldsymbol{\kappa}\cdot\mathbf{p}/(p^2+X^2)$ entering the corrections to the $\mathbf{A}\cdot\mathbf{P}$ contribution becomes

$$\frac{2\boldsymbol{\kappa}\cdot\mathbf{p}}{p^2+X^2}=\frac{p}{mc}\cos\theta. \tag{B17}$$

However, from Eq. (2),

$$\frac{p}{mc}=\sqrt{4\frac{\kappa}{mc}-(\alpha Z)^2}\approx\sqrt{4\frac{\kappa}{mc}}. \tag{B18}$$

This shows that the first corrections are proportional to $\sqrt{\kappa/mc}$, so they are rather large. They influence only the electron angular distribution because, when integrated over the electron direction, the corrections described in this section do not contribute.

[1] N. Berrah *et al.*, J. Mod. Opt. **57**, 1015 (2010).
[2] N. Rohringer *et al.*, Nature (London) **481**, 488 (2012).
[3] V. Richardson *et al.*, Phys. Rev. Lett. **105**, 013001 (2010).
[4] G. Doumy *et al.*, Phys. Rev. Lett. **106**, 083002 (2011).
[5] H. R. Varma, M. F. Ciappina, N. Rohringer, and R. Santra, Phys. Rev. A **80**, 053424 (2009).
[6] V. Florescu, O. Budriga, and H. Bachau, Phys. Rev. A **84**, 033425 (2011).
[7] M. Dondera and H. Bachau, Phys. Rev. A **85**, 013423 (2012).
[8] E. Karule, J. Phys. B **11**, 441 (1978).
[9] A. Maquet, V. Véniard, and T. Marian, J. Phys. B **31**, 3743 (1998).
[10] W. Zernik, Phys. Rev. **135**, A51 (1964).
[11] E. Arnous, S. Klarsfeld, and S. Wane, Phys. Rev. A **7**, 1559 (1973).
[12] S. Klarsfeld, Lett. Nuovo Cimento **2**, 548 (1969).
[13] M. Gavrila, Lett. Nuovo Cimento **2**, 180 (1969).
[14] M. Gavrila, Phys. Rev. A **6**, 1348 (1972).
[15] P. Koval, S. Fritzsche, and A. Surzhykov, J. Phys. B **36**, 873 (2003).
[16] P. Koval, S. Fritzsche, and A. Surzhykov, J. Phys. B **37**, 375 (2004).
[17] R. H. Pratt, in *X-Ray and Inner-Shell Processes*, 18th International Conference, edited by R. W. Dunford *et al.* (AIP, New York, 2000), p. 59.
[18] S. Klarsfeld, Lett. Nuovo Cimento **1**, 682 (1969).
[19] C. K. Au, Phys. Rev. A **14**, 531 (1976).
[20] M. Gavrila and A. Costescu, Phys. Rev. A **2**, 1752 (1970).
[21] L. Safari, P. Amaro, S. Fritzsche, J. P. Santos, and F. Fratini, Phys. Rev. A **85**, 043406 (2012).
[22] H. Bachau, O. Budriga, M. Dondera, and V. Florescu, Cent. Eur. J. Phys. (to be published, 2013).
[23] L. B. Madsen and P. Lambropoulos, Phys. Rev. A **59**, 4574 (1999).
[24] P. Appell and J. Kampe de Feriet, *Fonctions Hypergeometriques et Hyperspheriques* (Gauthtier-Villars, Paris, 1926).